

# Wear and Corrosion Resistant Amorphous / Nanostructured Steel Coatings For Replacement of Electrolytic Hard Chromium

**D.J. Branagan, M.C. Marshall, & B.E. Meacham,**  
*The NanoSteel Company*  
Idaho Falls, Idaho

**L. F. Aprigliano,**  
*Strategic Analysis, retired Naval Surface Warfare Center*  
West Bethesda, Maryland

**R. Bayles, E. J. Lemieux, T. Newbauer & F. J. Martin,**  
*Naval Research Laboratory & Geo-Centers Corporation*  
Washington, DC

**J. C. Farmer, J. J. Haslam, & S. D. Day,**  
*Lawrence Livermore National Laboratory, USDOE*  
Livermore, California

## Abstract

In severe corrosive or abrasive environments, steel is rarely used since the range of properties available, in existing steels, are insufficient, resulting in the prevalent usage of either corrosion resistant materials like nickel based superalloys or abrasion resistant materials like tungsten carbide based hardmetals. Recently, a host of carbide based alloys including WC-Co-Cr, NiCr-Cr<sub>3</sub>C<sub>2</sub>, WC-WB-Co etc. have been developed in an attempt to bridge the gap between providing both wear and corrosion protection [1,2]. Data will be presented showing how a newly developed steel coating, SAM2X5, with an amorphous / nanocomposite structure can bridge the gap between conventional metallic alloys and ceramic hardmetal performance with excellent combinations of properties including corrosion resistance superior to nickel base superalloys in seawater / chloride environments and wear resistance approaching that of tungsten carbide. The unique combination of damage tolerance developed should be especially applicable for the replacement of electrolytic hard chromium coatings.

## Introduction

Corrosion and wear occur on all exposed metallic surfaces and a wide variety of coating operations have been developed in an attempt to mitigate these problems. Electrolytic hard chrome coatings have gained widespread use within private industry and the US military due to its good tribological and electrochemical characteristics and historically low cost. Recently, OSHA proposed lowering the hexavalent chromium permissible exposure limit (PEL) from a ceiling concentration of 52 µg/m<sup>3</sup> to 1.0 µg/m<sup>3</sup> over an eight hour time weighted average [3]. A final standard in place from OSHA is expected at the end of 2005 and may significantly decrease the efficiency and increase the cost of electrolytic hard chrome plating [4]. While chromium is itself essentially inert, the primary problem

lies with the hard chrome plating process and the release of hexavalent chromium ions in which has long been known to be carcinogenic and other medical problems.

Hard chromium coatings are used in virtually all military applications which overhaul aircraft, land vehicles, and ships, and are part of extensive corrosion protection strategies employed by the United States Department of Defense, and involve several hundred thousand maintenance personnel. The High Performance Corrosion Resistant Material (HPCRM) Team was developed to address specific corrosion issues of interest to the United States Federal Government. A unique collaboration has been established between the Department of Energy (DOE) and the Defense Advanced Research Project Agency (DARPA) to meet the needs of both agencies. The data presented here is a subset of a much larger body of work that has been conducted by the HPCRM Team [5, 6]. Corrosion prevention applications are of primary interest to DARPA and the Navy, though there are numerous other applications. Materials such as these may also prove to be enabling in the general area of nuclear power generation. These newly developed materials and coatings provide naval architects and engineers with unique opportunities to simultaneously combat corrosion, corrosion-erosion and wear.

HVOF coatings are an alternative coating procedure to electrolytic hard chromium and can offer several advantages including much higher deposition rates, the elimination of hydrogen embrittlement issues, and the ability to repair in the field with systems that have already been deployed. The main issue with HVOF coatings is that often the corrosion resistance in coating form is much lower than the same respective material in plate form [7, 8]. In this paper, results will be given showing the damage tolerance of the newly developed SAM2X5 HVOF coatings which due to its combination of favorable properties may offer a very viable alternative for the replacement of electrolytic hard chromium, in line of site

applications for a wide variety of applications of interest to both the USDOE and USDOD.

### Experimental Procedure

The enabling ability to develop new coatings, which are iron based, yet which exhibit superior corrosion resistance is achieved by simultaneously reducing the scale of the microstructure while optimizing the passive protective oxide layer. A metallic glass which represents an angstrom scale material represents the ultimate in microstructural uniformity and exhibits a characteristic that during devitrification nanoscale structures result. Thus, the ability for a particular alloy composition to form a glass, i.e. its glass forming ability, is paramount to achieving significant improvements in properties. The SAM2X5 alloy is an 8 element Fe-Cr-Mo-W-Mn-B-C-Si material which was designed to have high glass forming ability and the ability to form an extremely passive Cr-Mo-W based oxide layer. Through detailed thermal analysis experiments this alloy was found to exhibit a reduced glass temperature of 0.57, a glass transition temperature 579°C, and a three stage crystallization with peaks at 630°C, 671°C, and 777°C. After argon atomization, the powder was sieved and air classified to yield feedstock powder nominally +15 to -53 µm in diameter, which had an appropriate distribution for spraying with the JP5000 gun system. The HVOF spray parameters used for the coatings are shown in Table 1.

Observation of the microstructure was conducted using a Hitachi S3000N Scanning Electron Microscope (SEM) with an EDAX Phoenix system. X-ray diffraction was done using a Phillips X'Pert MPD X-ray Diffractometer with scans that were nine hours in length in order to provide appropriate peak to background resolution for Rietveld refinement to identify phases. The density of the SAM2X5 coupons was measured using Image-pro plus version 3.0.1 Media Cybernetics metallographic software. Cyclic polarization measurements were based on a procedure similar to ASTM G 5, and were conducted in Half Moon Bay seawater at 30°C and 90°C. Corrosion rates were determined with linear polarization of samples with a 600-grit finish. Salt fog testing was conducted according to the ASTM B117 "Standard Test Method of Salt Spray (Fog) Testing" using the GM9540P protocol. Note that each cycle of testing represents exposure in the Salt Fog chamber of 24 hours. Vickers microhardness measurements were made on the cross section of the HVOF coatings at 300 gram load and reported as an average of 5 measurements. The wear resistance was determined using the ASTM G-65 Dry Sand Rubber Wheel Abrasion Testing using Procedure A with a total test duration of 6,000 cycles.

Table 1: HVOF Spray Parameters.

Experimental	Parameter Used
HVOF Gun System	Tafa JP5000 with 4" barrel
Stoichiometric Ratio (Equivalence Ratio)	105% (0.95)
Combustion Pressure	90 psig
Powder Feeder	Miller / Praxair model 1270
Powder Feed RPM	4 with a 6 slm argon carrier gas
Coating Thickness	Nominally 15 mils (375 µm)
Traverse Speed / pitch	100 mm/sec / 5 mm with a 350 mm coupon stand-off
Sample Preparation	Grit blasted with 24 Alundum at 100 psi / rinsed with methanol

### Results and Discussion

#### Coating Structure

After optimization of the spray parameters, the cross section structure of the SAM2X5 coatings can be seen in Fig. 1. In Fig. 1a, the optical micrograph is shown of the entire cross section which shows that a very high coating density has been achieved which has been estimated to be 99.7%. In Fig. 1b, a close-up of the cross section is shown using backscattered electrons in the SEM. While the macrostructure of the coating can be seen, the microstructure is not evident since it is found to be smaller than the resolution in the SEM.

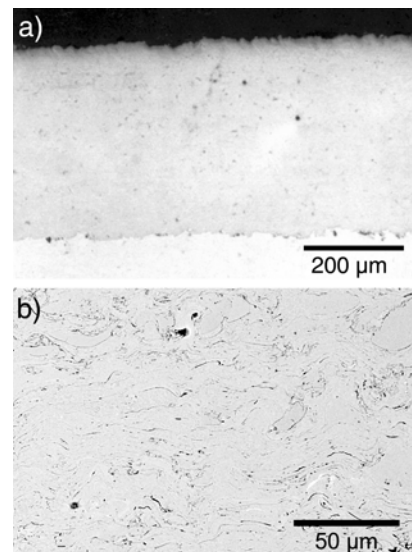


Figure 1: Micrographs of the SAM2X5 coatings in the as-sprayed condition; a) Optical micrograph, B) SEM backscattered micrograph.

The structure of the SAM2X5 coatings were analyzed primarily using X-ray diffraction. In Fig. 2, the as-sprayed HVOF coating is shown. The broad amorphous humps and lack of Bragg diffraction peaks (even after a 9 hour scan) are indicative of an amorphous structure and verify that the as-sprayed coating's structure is primarily a metallic glass. Metallic glass coatings can be subsequently heat treated above their crystallization temperature to cause the solid solid state devitrification transformation in order to form nanocomposite coatings [9, 10]. After heat treating at 800°C for 10 minutes to fully devitrify the coating, an X-ray scan was taken to identify the crystalline phases which formed. The experimental pattern and the Rietveld refined pattern with an excellent fit are shown in Fig. 3. Three phases were identified including  $\alpha$ -Fe (ferrite) with a space group of Im-3m and lattice parameter  $a = 0.2878$  nm,  $\gamma$ -Fe (austenite) with a space group of Fm-3m and lattice parameter  $a = 0.3602$  nm, and a borocarbide phase  $M_{23}(BC)_6$  with a space group of Fm-3m and lattice parameter  $a = 1.1054$  nm.

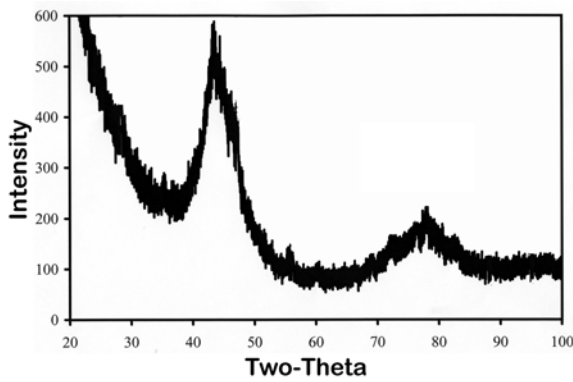


Figure 2: X-ray diffraction diagram of the as-sprayed SAM2X5 HVOF coating.

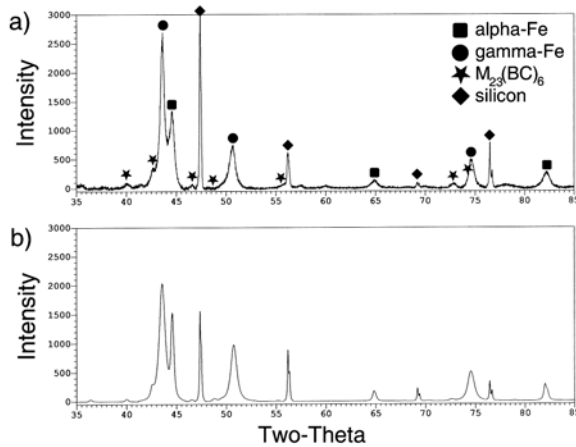


Figure 3: X-ray diffraction diagrams of the SAM2X5 HVOF coating which was heat treated at 800°C for 10 minutes: a) Experimental pattern with peaks identified, b) Rietveld refined pattern.

#### Hardness / Wear Resistance

The hardness of the SAM2X5 coatings along with the baseline 316L and C-22 coatings were measured in the as-sprayed and heat treated (700°C for 10 minutes) conditions (Fig. 4). The SAM2X5 as-sprayed coatings were found to have hardness values which ranged from 981 to 1062 kg/mm<sup>2</sup>. After heat treatment, the hardness of the SAM2X5 coating was found to increase significantly with hardness values which ranged from 1178 to 1293 kg/mm<sup>2</sup>. The reason for this increase in hardness was that the glass content in the coating was able to fully devitrify and form a harder nanocomposite structure containing  $M_{23}(BC)_6$  borocarbide phases. In contrast, note that the hardness values for the 316L and C-22 coatings were comparatively very low with HV300 averages at 286 kg/mm<sup>2</sup> and 377 kg/mm<sup>2</sup> respectively. After heat treatment, the hardness of the 316L and C-22 coatings were found to only increase marginally, which is not surprising since they do not contain glass and therefore cannot devitrify.

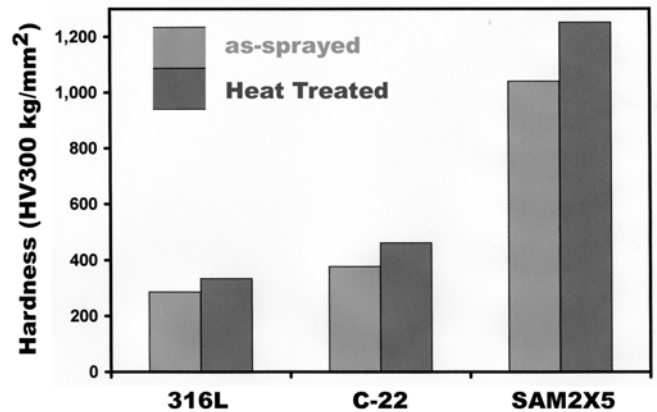


Figure 4: Average Vickers hardness (HV300) for the coatings in the as-sprayed and heat treated condition.

To test the wear resistance, HVOF coupons of each alloy in both the as-sprayed and heat treated (700°C for 10 minutes) conditions were tested using the ASTM G-65 Dry Sand Rubber Wheel Abrasion Test. As shown in Fig. 5, the SAM2X5 HVOF coatings experience a wear resistance which is far superior to C-22 and 316L coatings, which are normally used for corrosion resistance. Note that for the 316L, C-22, that the heat treatment caused little change in wear rate but for the SAM2X5 coating the wear resistance was increased by more than double, due to the devitrification.

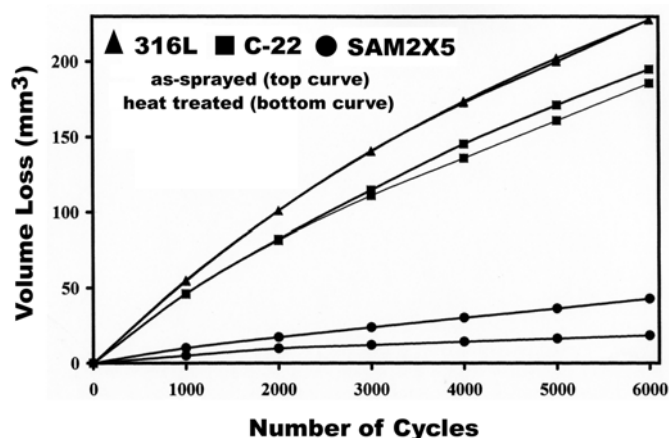


Figure 5: ASTM G-65 Procedure A volume loss for the 316L, C-22, and SAM2X5 coatings in the as-sprayed and heat treated condition.

### Electrochemical / Corrosion Resistance

Cyclic polarization testing measurements were used as a means of measuring the critical potential of the corrosion-resistant outer layer ( $E_{crit}$ ), relative to the open-circuit corrosion potential ( $E_{corr}$ ). Spontaneous breakdown of the passive film and localized corrosion require that the open-circuit corrosion potential exceed the critical potential (i.e.  $E_{CORR} > E_{CRIT}$ ). After a 24-hour hold period, during which the open circuit corrosion potential is determined, the potential was scanned in the positive (anodic) direction from a level slightly more negative than the corrosion potential (cathodic limit), to a reversal potential ( $E_{rev}$ ) near that required for oxygen evolution (anodic level). As the scan continues, the current density may eventually decrease to a level equivalent to that experienced during the positive scan, and indicative of reformation of the passive film. The potential at which this occurs is known as the repassivation potential ( $E_{rp}$ ). Large anodic values of the repassivation potential, relative to the open circuit corrosion potential, are indicative of a high degree of passive film stability, and substantial resistance to localized attack from pitting and crevice corrosion. Such behavior is attributed to inherent thermochemical stability of the oxide that covers the surface, as well as facile film formation kinetics for the oxide at the potential where repassivation forms. Cyclic polarization data for wrought plates and thermally sprayed samples in 30 and 90°C seawater are summarized in Tables 2 and 3. All samples were polished to a 600-grit finish prior to testing. Three characteristic quantities are shown, the open-circuit corrosion potential ( $E_{corr}$ ), the repassivation potential ( $E_{rp}$ ), and the difference between  $E_{corr}$  and  $E_{rp}$ , represented by  $\Delta E$ . Thermally sprayed iron-based amorphous metals such as newly developed SAM2X5 have relatively high differential potentials ( $\Delta E$ ) in comparison to those measured for wrought plates of Type 316L stainless steel and nickel-based Alloy C-22, and thermally sprayed Alloy C-22. During electrochemical testing, it was found that the passive oxide film reformed readily on thermally sprayed SAM2X5, with corresponding repassivation potentials of 760 and 700 mV, respectively. All potentials were

measured relative to a standard Ag/AgCl reference electrode, maintained at 25°C with active cooling, and filled with saturated KCl electrolyte. The reference electrode communicated with the test solutions via Luggin probes. Potential corrections for the junction have been found to be relatively insignificant.

Table 2: Corrosion Results in Seawater at 30°C.

Alloy	Form	$E_{corr}$	$E_{rp}$	$\Delta E$
mV vs. Ag/AgCl				
316L	Wrought	-230	$< E_{corr}$	$< 0$
C-22	Wrought	-330	-690	+360
C-22	HVOF	-390	-130	+260
SAM2X5	HVOF	-110	+760	+870

Table 3: Corrosion Results in Seawater at 90°C.

Alloy	Form	$E_{corr}$	$E_{rp}$	$\Delta E$
mV vs. Ag/AgCl				
316L	Wrought	-210	-80	+130
C-22	Wrought	-320	-510	+190
C-22	HVOF	-580	-280	+300
SAM2X5	HVOF	-150	+700	+850

The critical potential,  $E_{crit}$ , was determined with potentiostatic step testing. The critical potential is also known as the “threshold” or “breakdown” potential, and was determined by monitoring the corresponding current density transient for durations ranging from 1 to 24 hours. In cases where passivity was lost, large anodic (positive) excursions of current density (dissolution) were observed. In cases where passivity was maintained, the current density decayed to a low, asymptotic value, indicative of the passive current density (approximately 1-2  $\mu\text{A}/\text{cm}^2$ ). The results of the threshold potential testing in seawater at 90°C are given in Table 4. While the current density of the Alloy C-22 thermal spray (HVOF) coating exceeded the 1-2  $\mu\text{A}/\text{cm}^2$  criteria at the lowest applied potential, the wrought C-22 plate did not exceed this until the potential was increased from 200 to 300 mV versus the open circuit corrosion potential. This clearly shows how corrosion resistance can be reduced during the thermal spraying process. In contrast, in the SAM2X5 coating, the passivity is maintained and the threshold potential is very high at 415 mV ( $\leq 415$  mV vs.  $E_{corr}$ ).

Table 4: Threshold Potential in Seawater at 90 °C.

Material / Sample	$E_{th}$ vs $E_{corr}$ (mV)
C-22 HVOF Coating	< 100
C-22 Wrought Plate	200 to 300
SAM2X5 HVOF Coating	415

Thus, thermally spray coatings of iron-based SAM2X5 amorphous metal exhibited substantially better passive film stability than wrought nickel-based Alloy C-22. Furthermore, while an Alloy C-22 powder loses most of its corrosion resistance during thermal spraying, which is believed to be due to the precipitation of well-known TCP phases, the iron-based amorphous metals such as SAM2X5 maintain a relatively high degree of corrosion resistance. Thus, for the first time, these new thermally sprayed materials provide the materials engineer with truly corrosion-resistant metal coatings.

For hard chrome replacement, HVOF coatings would generally be ground / polished, but other usages of advanced coatings would not require finishing so the response of the as-sprayed coatings is also of interest. Such data is shown in Fig. 6, where hysteresis loops are presented for the SAM2X5 coating and C-22 wrought plate in seawater at 90°C. The passive film on Alloy C-22 breaks down at the reversal potential of 1 volt during the anodic (forward) potential scan and the passive film breakdown causes the large hysteresis loop and no repassivation of the Alloy C-22 during the cathodic (reverse) potential scan. In contrast, the potential of the HVOF SAM2X5 coating can be scanned to 1.2 volts, close to oxygen evolution, with only a slight hysteresis loop, and a clear repassivation potential (intersection of forward and reverse scans) between 0.7 and 0.8 volts. Under these test conditions, the HVOF SAM2X5 coating is found to be far more resistant to corrosive attack in near-boiling seawater than the C-22 wrought plate.

In addition to having exceptional resistance to localized corrosion in seawater, which is reflected in the measurements of corrosion and repassivation potential, the corrosion rates of SAM2X5 are comparable to that of wrought Alloy C-22. These corrosion rates were determined from linear polarization measurements, and are shown in Table 5. Note that 1 mpy (millimicron per year) is equivalent to a penetration of  $1 \times 10^{-7}$  centimeters per year. In marine environments, these thermal spray coatings would be expected to exhibit very low penetration due to general corrosion.

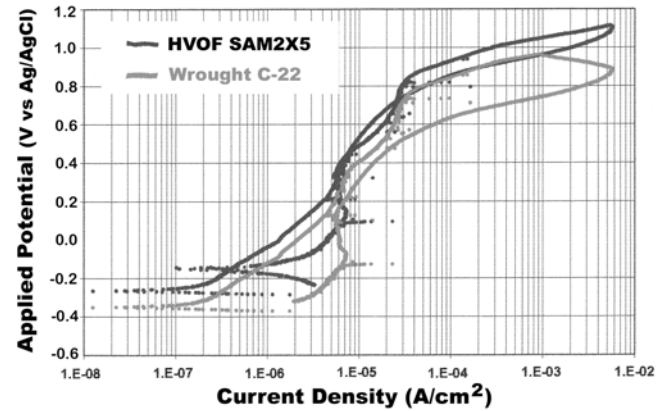


Figure 6: Comparison of cyclic polarization data for as-deposited thermal spray coating of SAM2X5 and wrought nickel-based C-22 in seawater at 90°C.

Table 5: Corrosion Rates in Seawater.

Alloy	Form	Temp. (°C)	Corrosion Rate (mpy)	Standard Deviation (Mmpy)
C-22	Wrought	30	83	3
SAM2X5	HVOF	30	250	150
C-22	Wrought	90	3000	20
SAM2X5	HVOF	90	2200	190

The standard ASTM B117 salt fog test a very severe test for any coating since coatings may not fully dense, and salt solution can communicate with the underlying substrate through interconnected porosity. Furthermore, pores in metal coatings may behave like pits, resulting in the lowering of pH within these occluded regions due to hydrolysis reactions involving dissolved divalent cations such as ferrous ion. The results of salt fog testing for 316L, C-22, and SAM2X5 coatings, which were all sprayed onto 316L substrates, are shown in Fig. 7. Corrosion was found on the 316L and C-22 coatings after 13 cycles of exposure. No corrosion was found to initiate on the SAM2X5 coatings after 28 cycles (672 hours) of exposure at the time the photograph was taken. Subsequent testing found no corrosion initiation of the SAM2X5 HVOF coatings after total exposure of 54 cycles (1296 hours) in the salt fog chamber. Also, due to the high density of the SAM2X5 coating, no bleedthrough was found either from the 316L wrought steel substrate.

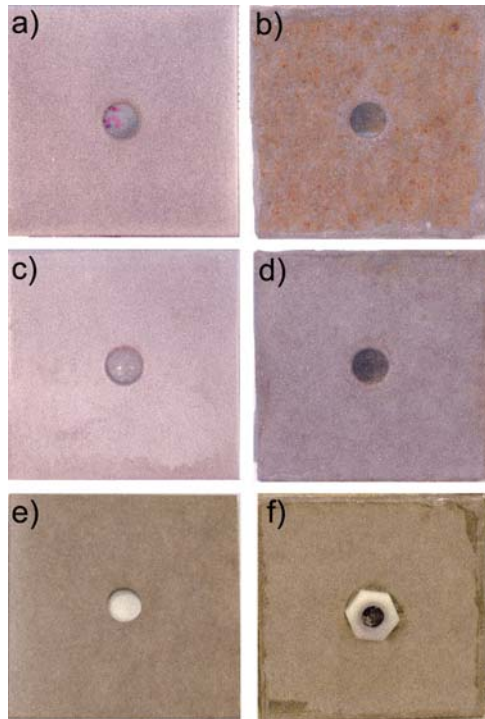


Figure 7: Results of ASTM B117 salt fog testing on HVOF coatings; a) 316L as-received, b) 316L after 13 cycles of exposure, c) C-22 as-received, d) C-22 after 13 cycles of exposure, e) SAM2X5 as-received, and f) SAM2X5 after 28 cycles of exposure.

### Conclusions

A new iron-based alloy was developed which readily forms amorphous or primarily amorphous coatings when thermal sprayed using the HVOF process. After heat treating above the glass crystallization peaks, the coating can be devitrified to a multiphase nanoscale composite microstructure. While conventional high corrosion materials in coating form, exhibit reduced corrosion behavior compared to their wrought counterparts, the newly developed SAM2X5 coatings are found to exhibit excellent corrosion resistance in seawater solutions and the salt fog environment. Its resistance is even found to be superior to wrought C-22 plate in the environments tested. Furthermore, while conventional corrosion materials are soft, the SAM2X5 coatings are found to be hard and wear resistant, roughly equivalent to hard chrome in the as-sprayed condition while approaching that of WC-Co in the devitrified condition. The excellent combination of properties allow this coating material to have excellent damage tolerance and should allow this material as a viable alternative for the replacement of electrolytic hard chrome for a wide range of industrial, governmental, or military applications.

### Acknowledgement

Work was sponsored by the Defense Advanced Research Projects Agency (DARPA) Defense Science Office (DSO) and the United States Department of Energy (DOE) Office of Civilian and Radioactive Waste Management (OCRWM). This work was done under the auspices of the U.S. DOE by Lawrence Livermore National Laboratory (LLNL) under Contract No. W-7405-Eng-48. The HPCRMT Team expresses their gratitude to sponsors for financial support, and supportive colleagues for making this work possible. This document has been approved for Public Release, Distribution Unlimited.

### References

1. A. Kirsten, M. Oechsle, and R.F. Moll, Carbide Containing Materials For Hard Chromium Replacement by HVOF-Spraying, *ITSC 2005 Proc.*, Basel, Switzerland, May 2-4, 2005, ASM Int., p957-962.
2. S. Bouaricha, J.-G. Legoux and B.R. Marple, HVOF Coatings Properties of the Newly Thermal Spray Composition WC-WB-Co, *ITSC 2005 Proc.*, Basel, Switzerland, May 2-4, 2005, ASM Int., p981-985.
3. Proposed Rule, "Occupational Exposure to Hexavalent Chromium", *Federal Register*, Vol. 69, No.191, October 4, 2004, p59,306.
4. Keith Legg, "Alternative Technologies for Corrosion Prevention – An Analytical Toolkit", *Proceedings of 1<sup>st</sup> World Congress on Corrosion in The Military*, Sorrento, Italy, June 2005.
5. Farmer et al., Corrosion Characterization of Iron-Based High-Performance Amorphous-Metal Thermal-Spray Coatings, *Proceedings of ASME PVP Division Conference*, July 17 - 21, 2005 Denver, CO, PVP2005-71664, American Society of Mechanical Engineers, 7 pages.
6. Farmer et al., High-Performance Corrosion-Resistant Materials: Iron-Based Amorphous-Metal Thermal-Spray Coatings, UCRL-TR-206717, Lawrence Livermore National Laboratory, September 28, 2004, 178 pages.
7. S. Shrestha and A.J. Sturgeon, "Use Of Advanced Thermal Spray Processes For Corrosion Protection In Marine Environments", *Surface Engineering*, 20(2004), p237-243.
8. Petri Vuoristo and Jorma Vihinen, "High-Performance Laser Coatings For Manufacturing and Maintenance of Industrial Components and Equipment", *Kunnossapito*, 5(2002), p2-8.
9. D.J. Branagan, "Formation of Nanoscale Composite Coating Via HVOF and Wire-Arc Spraying", *ITSC 2005*, Basel, Switzerland, May 2-4, 2005, p 539-544.
10. D.J. Branagan, W.D. Swank, D.C. Haggard, J.R. Fincke, "Wear Resistant Amorphous and Nanocomposite Steel Coatings", *Metallurgical and Materials Transactions A*, 32A (2001), p2615-2621.